Plant Soil (2016) 398:87–97
DOI 10.1007/s11104-015-2627-x

REGULAR ARTICLE

The influence of iron plaque on the absorption, translocation and transformation of mercury in rice (*Oryza sativa* L.) seedlings exposed to different mercury species

Yunyun Li · Jiating Zhao · Bowen Zhang · Yongjie Liu · Xiaohan Xu · Yu-Feng Li · Bai Li · Yuxi Gao · Zhifang Chai

Received: 16 March 2015 / Accepted: 31 July 2015 / Published online: 22 August 2015

Abstract

Background and aims Iron plaque can affect the absorption and accumulation of metal(loid)s in plants. However, it is still unclear whether iron plaque plays different roles in the accumulation of different mercury species in rice plants. The aims of this study are 1) to explore the adsorption of IHg and MeHg onto iron plaque, 2) to investigate the influence of iron plaque on the absorption, translocation of IHg and MeHg in rice plants, 3) to explore whether the process of methylation and demethylation of Hg in vivo occurs in rice plants, and 4) to investigate the effects of iron plaque on the IHg and MeHg transformation in rice.

Methods The seedlings were cultivated in an Fe^{2+} solution for 24 h to induce the iron plaque and then transferred into a nutrient solution containing 500 μg/L $HgCl_2$ or MeHgCl for 72 h. The Hg content in the iron plaque and rice seedlings was measured by ICP-MS. The chemical forms of Hg in the rice seedlings were determined with HPLC-ICP-MS and XANES.

Results Both IHg and MeHg, particularly MeHg, could be adsorbed by iron plaque. The IHg content of the root and the MeHg content in both the roots and shoots decreased markedly with the increase in iron plaque. The Hg in the root was mainly in the form of RS-Hg-SR with the exposure to $HgCl_2$ and in the form of CH_3-Hg-SR and RS-Hg-SR (4:1) with the exposure to MeHgCl. The iron plaque did not change the chemical forms of Hg in the rice plants.

Conclusions Iron plaque greatly decreased the absorption and translocation of both IHg and MeHg in rice seedlings. The demethylation of MeHg occurred in rice plants (in vivo) regardless the formation of iron plaque. This work sheds some light on the understanding of different pathways between IHg and MeHg in rice plants.

Keywords Inorganic mercury · Methylmercury · Iron plaque · Rice · Demethylation

Responsible Editor: Henk Schat.

Y. Li · J. Zhao · B. Zhang · Y. Liu · X. Xu · Y.-F. Li · B. Li · Y. Gao (✉) · Z. Chai
CAS Key Laboratory for Biomedical Effects of Nanomaterials and Nanosafety, and Laboratory of Metallomics, Institute of High Energy Physics, Chinese Academy of Sciences, Beijing 100049, China
e-mail: gaoyx@ihep.ac.cn

Y. Li · X. Xu
University of Chinese Academy of Sciences, Beijing 100049, China

B. Zhang
Department of Basic Medicine, Baotou Medical College, Baotou 014010, China

Y. Liu
Forestry College, Shanxi Agricultural University, Taigu, Shanxi 030801, China

Introduction

Mercury (Hg) and its compounds are listed as priority pollutants by many international organizations because

of their high toxicity, persistence in the environment, and bioaccumulation in the food chain (Clarkson and Magos 2006; Jiang et al. 2006; Syversen and Kaur 2012). Because of coal combustion, mining and smelting of Hg and other nonferrous metals, together with industrial and agricultural activities, soils have been severely polluted by Hg in some areas of China (Horvat et al. 2003; Jiang et al. 2006). For example, in the surrounding soil of the Wuchuan Hg Mine the total Hg content of ranged from 0.33 to 320 mg/kg and the total content MeHg ranged from 0.69 to 20 μg/kg (Qiu et al. 2006), which far exceed the Chinese national limit for paddy soils (1.5 mg/kg) (GB15618-1995). The Hg pollution in the soil will directly affect the production and quality of agricultural products. Rice (*Oryza sativa* L.) is a staple cereal worldwide, especially in Asia. It was reported that the contents of inorganic mercury (IHg) and methylmercury (MeHg) in rice grain were 94 (7.4~460) μg/kg and 11 (1.2~44) μg/kg in a Hg-polluted area (Zhang et al. 2010), which is higher than the limit of the Chinese national standards for the cereal (20 μg/kg, GB2762-2005). Rice consumption has become the main source of MeHg exposure for local residents, which poses potential health risks to them (Wang et al. 2011; Zhao et al. 2009).

The toxicity of Hg largely depends on its chemical forms. MeHg is regarded as the most toxic form due to its tendency for bioaccumulation and biomagnification through the food chain and transportation across the blood–brain barrier (Diez 2009; Syversen and Kaur 2012; Wei et al. 2014). Our previous work revealed that the proportion of MeHg to total Hg in rice grain was as high as 50 % (Zhao et al. 2014), which raised a great concern for the rice-dependent populations in Hg-contaminated areas. Microbes have been considered the main producers of MeHg in an anoxic environment, such as sediment or swampland (Benoit et al. 2003; Wei et al. 2013). Paddy fields are a unique ecosystem, possessing both the characteristic of aquatic and terrestrial ecosystems. Therefore, Hg is also methylated in the paddy, and paddies have been perceived as the main source of MeHg in rice (Li et al. 2010). Some reports have recently shown that there is Hg methylation in some kinds of fish (Wang et al. 2013) and aquatic plants (Deng et al. 2013). The demethylation of MeHg could occur in the liver of marine mammals (Khan and Wang 2009). Therefore, whether the process of IHg methylation or MeHg de-methylation occurs in rice plants deserves further study.

Iron plaque is commonly formed on the root surface of many aquatic plant species, which helps plants adapt to aquatic environmental stress (Fu et al. 2010; Li et al. 2014). It can affect the bioavailability and migration of metal(loid)s through absorption-desorption, oxidation-reduction, organic–inorganic chelation, co-precipitation, and so on. (He et al. 2004; Liu et al. 2014; Tripathi et al. 2014). The role of iron plaque in the uptake of different elements in rice plants has been investigated in several studies (Hu et al. 2014; Huang et al. 2012; Lee et al. 2013; Liu et al. 2008). The formation of iron plaque has been found to sequester arsenic (As) and reduce its uptake by rice from the culture medium (Lee et al. 2013; Syu et al. 2013, 2014). Other studies have found that iron plaque can immobilize chromium (Cr) from the environment but not significantly affect the Cr uptake and translocation in rice seedlings (Hu et al. 2013, 2014). Wang et al. (2014) found that the amount of Hg in straw and brown rice negatively correlated with iron plaque, suggesting that iron plaque could reduce the accumulation of Hg in rice plants. However, it is still unclear whether the formation of iron plaque plays a different role in the absorption, translocation and transformation of different Hg species, i.e., IHg and MeHg in rice plants. The aims of this study are 1) to explore the adsorption of IHg and MeHg onto iron plaque, 2) to investigate the influence of iron plaque on the absorption, translocation of IHg and MeHg in rice plants, 3) to explore whether the process of methylation and demethylation of Hg in vivo occurs in rice plants, and 4) to investigate the effects of iron plaque on IHg and MeHg transformation in rice.

Materials and methods

Rice cultivation

Rice seeds (*Oryza sativa* L.GY1255) were disinfected with 1 % (*V/V*) sodium hypochlorite (NaClO) solution for 15 min and then washed thoroughly with deionized water (18.2 MΩ·cm). The seeds were germinated in moist perlite at 28 °C in the dark for 1 week. Uniform seedlings were selected and cultivated in a 300 mL 25 % Hogland solution (pH=5.0) for 3 weeks. The nutrient solution was renewed twice a week. All of the plants were cultured in a man-made climate growth chamber with a 14 h light period (300–350 μmol/m^2/s, 28 °C, humidity 60 %) and a 10 h dark period (20 °C, humidity 70 %).

Induction of iron plaque and exposure to Hg

All rice seedlings were transported into a 0.5 mmol/L $CaCl_2$ (pH=5.5) solution for 2 h to minimize the interference of Fe from other elements. Iron plaque was induced by exposing the rice roots to 0, 20, 50, 80, 100 mg/L of ferrous ions ($FeSO_4 \cdot 7H_2O$) for 24 h, assigned as the Fe0, Fe20, Fe50, Fe80, and Fe100 groups, respectively. The rice seedlings were then transferred into a 25 % Hogland solution for another 48 h and then into a nutrient solution containing 500 μg/L $HgCl_2$ or MeHgCl for 72 h. Afterwards, the rice seedlings were harvested and the nutrient solutions were collected.

Extraction of iron plaque and analysis of Fe content

The iron plaque on the root surface was extracted with a dithionite–citrate–bicarbonate method (DCB) (Huang et al. 2012). The entire roots were washed thoroughly with deionized water prior to the incubation in a 30 mL solution containing 0.5 g sodium dithionite ($Na_2S_2O_4$), 0.03 mol/L sodium citrate ($Na_3C_6H_5O_7 \cdot 2H_2O$), and 0.125 mol/L sodium bicarbonate ($NaHCO_3$) at room temperature for 1 h. The roots were then rinsed three times with deionized water. Finally, the DCB extracts were diluted to 50 mL with deionized water. After DCB extraction, the roots and shoots were air dried to constant weight.

The Fe concentration in the DCB extractions was determined with an Inductively Coupled Plasma Optical Emission Spectrometer (ICP-OES, Optima 2000DV, PerkinElmer, USA). The working conditions of the ICP-OES were as follows: forward power (1300 W), observation height (15 mm), plasma gas flow rate (0.8 L/min), and injection volume (1.5 mL/min).

Analysis of Hg content in the DCB extractions, roots and shoots

The dried roots and shoots were ground into a fine powder with a mortar and pestle. The root and shoot powders (approximately 50 mg) were mixed with 5 mL HNO_3 (BV-III) and 1 mL H_2O_2 (MOS). The mixtures were left overnight at room temperature and then digested at 160 °C in high pressure Teflon digestion vessels for 6 h. Afterwards, the mixtures were evaporated to approximately 1 mL at 90 °C. The residual solution was diluted to 5 mL with 2 % (*V/V*) HNO_3 containing 0.1 % (*V/V*) β-mercaptoethanol. The Hg calibration standard was prepared by diluting the Hg standard stock solution (GBW 08617, National Research Centre for CRMs, China) with 2 % (*V/V*) HNO_3 containing 0.1 % (*V/V*) β-mercaptoethanol. The Hg in the DCB extracts and rice tissues was determined using inductively coupled plasma mass spectrometry (ICP-MS, Thermo Elemental X7, USA) in standard mode. Instrument optimization was performed every time with a normal tuning solution (Bi 20 ppb). The working conditions of the ICP-MS were as follows: forward power (1300 W), plasma gas flow rate (13.0 L/min), auxiliary gas flow rate (0.8 L/min), nebulizer gas flow rate (0.72 L/min), and sample uptake rate (0.8 mL/min).

Analysis of Hg speciation with HPLC-ICP-MS

The IHg and MeHg contents in the rice tissues were analyzed with an HPLC-ICP-MS hyphened technique according to Zhao et al. (2014). The powder of the roots or shoots (approximately 50 mg) was treated with 5 mL 6 mol/L HCl. The mixtures were shaken overnight at room temperature after 1 h of ultrasonic vibration. Then, the mixtures were centrifuged at 10000 r/min (Eppendorf, Germany) for 10 min. The supernatant was collected and adjusted to a pH of 6.7 with ammonia and diluted to 10 mL with the mobile phase (pH=6.7) containing 0.06 mol/L ammonium acetate, 5 % (*V/V*) methanol and 0.3 % (*V/V*) β-mercaptoethanol. All of the solutions were filtered using a 0.22 μm microporous membrane filter before analysis. A liquid chromatography pump (WAT055028 metal-free 626 pump, Waters, Milford, USA) and a 5 μm Symmetryshield RP18 column (150× 3.9 mm, Waters, Milford, USA) were used to separate IHg and MeHg. The injection volume was 100 μL, and the flow rate was 1 mL/min. The Hg speciation in the nutrient solution was analyzed with the same procedure. The calibration standards of IHg and MeHg were prepared by diluting the IHg standard stock solution (GBW 08617, National Research Centre for CRMs, China) and MeHg standard stock solution (GBW 08675, National Research Centre for CRMs, China) with the mobile phase.

Distribution of Fe and Hg in iron plaque with μ-SRXRF

Fresh rice roots were immersed in the embedding agent (SAKURA Tissue-Tek OCT) and frozen at −80 °C. Then, the roots were cut into 40 μm-thick slices with a freezing microtome (Reichert-Jung, Germany). The slices were placed on Mylar films (polycarbonate) and then dried and stored at −20 °C prior to the micro beam-

synchrotron radiation X-ray fluorescence (μ-SRXRF) analysis. Fresh rice roots were also placed between two layers of cellophane and dried using Gel Drier (Bio-Rad) for the measurement of element distribution in the longitudinal section of the root.

The Fe and Hg distributions in the cross and longitudinal section were measured at BL15U at the Shanghai Synchrotron Radiation Facility (SSRF, China), in which the storage ring runs at 3.5 GeV with a current intensity from 200 mA to 300 mA. The incident X-ray energy of 13 keV was monochromatized by a Si(111) double-crystal monochromator and focused to a spot size of 5×5 μm^2 with a K-B system. The rice root slices were fixed on a precision motor-driven stage. The fluorescence signals from the slices were recorded and analyzed with a 7 element Si(Li) detector combined with a multiple channel analyzer (e2v, UK). The sample platform was moved along the horizontal and perpendicular direction at an interval of 5 μm for each step. The count time was 1.5 s per pixel. The peak areas of the elements were normalized to the current intensity (I_0) in the ionization chamber to correct for the effect of SR beam flux variation on the signal intensity.

Chemical forms of Hg in rice plants with XANES

A Hg L_3-edge X-ray absorption near-edge structure spectroscopy (XANES) experiment was conducted at the 1W1B beamline at the Beijing Synchrotron Radiation Facility (BSRF). The storage ring was at 2.5 GeV with a maximum current intensity of approximately 250 mA. A Si(111) double-crystal monochromator was detuned to minimize the harmonic content of the beam. After the iron plaque extraction, the rice roots were ground into a fine powder, which was smeared onto Scotch tape. The Hg L_3-edge XANES spectra were collected at room temperature in fluorescence mode for all plant samples and in transmission mode for all Hg reference compounds including HgS, $HgCl_2$, Hg-glutathione ($Hg(GS)_2$), CH_3HgCl, CH_3HgGS. The data was normalized and analyzed using the IFEFFIT program.

Results

Formation and distribution of iron plaque on roots

Reddish iron plaque on the root surface became visible after 24 h of incubation in a solution with different Fe^{2+} concentrations, but it was not observed on the rice without the Fe^{2+} treatment. The Fe concentration in the DCB extracts was used to represent the amount of iron plaque. Figure 1 illustrated the relationship between the amount of iron plaque and the Fe concentration in the pretreatment solutions. The formation of iron plaque was markedly affected by the Fe addition. The amount of iron plaque increased with the increasing Fe^{2+} concentrations in the 0-80 mg/L of Fe^{2+} pretreatment solutions and then stabilized.

Figure 2 shows the micrographs and the mapping of Fe in the cross and longitudinal sections of the rice tissues imaged with μ-SRXRF. The Fe was concentrated on the root surface when the rice was treated with 80 mg/L of Fe^{2+} (Fig. $2b_1$ and d_1). Little Fe was found on the root surface without the Fe^{2+} treatment (Fig. $2a_1$ and c_1) in contrast with the root surfaces treated with 80 mg/L of Fe^{2+} (Fig. $2b_1$ and d_1). From Fig. 2f,we can see that the iron plaque was mainly deposited in the maturation zone of the root (Fig. 2f). Only a small amount of iron plaque was formed on the root tip.

Hg adsorption in iron plaque and distribution in rice roots

The amounts of IHg and MeHg adsorbed in iron plaque were investigated by measuring the Hg concentrations in the DCB extracts. The results are shown in Fig. 3. The Hg concentration in the DCB extracts increased dramatically with the amount of iron plaque, ranging from 34.64±6.59 to 114.41±3.71 mg/kg for $HgCl_2$ exposure and from 86.67±14.09 to 287.67±

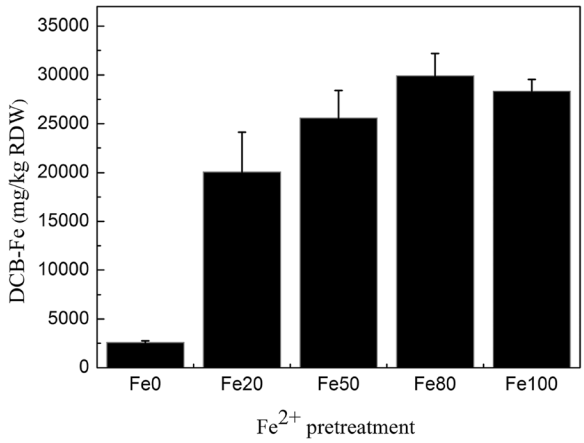

Fig. 1 The influence of Fe^{2+} concentration in the pretreatment solution on the amounts of iron plaque formed on the root surface. (Means±SD, n=3)

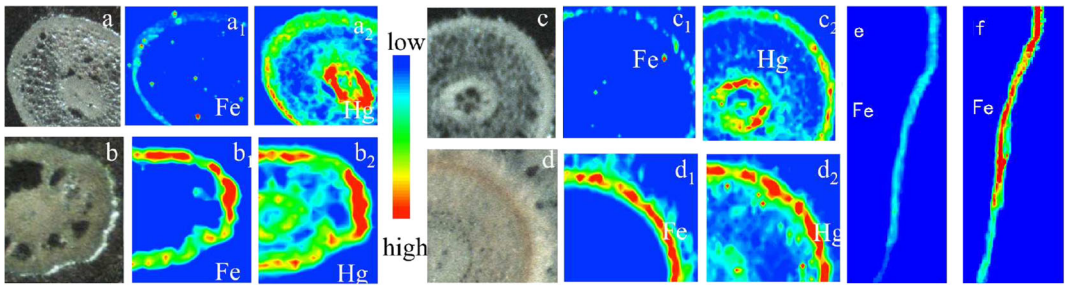

Fig. 2 The distribution of Fe and Hg in the root tissues of rice measured by μ-SRXRF. Left, the element distribution on a cross section of the root under IHg exposure, without (**a**) or with (**b**) iron plaque induction ($\mathbf{a_1}$ and $\mathbf{b_1}$ for Fe; $\mathbf{a_2}$ and $\mathbf{b_2}$ For Hg); right, the cross section of the root tissues from rice without (**c**) or with (**d**) iron plaque induction under MeHg exposure ($\mathbf{c_1}$ and $\mathbf{d_1}$: Fe XRF image; $\mathbf{c_2}$ and $\mathbf{d_2}$: Hg XRF image); and Fe distribution in the longitudinal section of rice tissues without (**e**) or with (**f**) iron plaque induction

39.66 mg/kg for MeHg exposure (Fig. 3). The Hg content in the iron plaque exposed to MeHg was twice that of the iron plaques exposed to IHg. Hence, the iron plaque adsorbed both Hg species, especially MeHg. A strong positive correlation (r^2=0.790 for IHg, r^2=0.852 for MeHg) between the Hg and Fe concentrations in the DCB extracts was found under IHg and MeHg exposure (Fig. 3).

The Hg distribution in the rice roots was measured using μ-SRXRF. The result is shown in Fig. 2. The Hg was mainly concentrated in the epidermis, endodermis and vascular tissues. An increase in Hg accumulation in the epidermis and a decrease in Hg enrichment in the pericycle were found (as shown in Fig. $2b_2$ and d_2) with the Fe^{2+} treatment.

Hg content in the roots and shoots

The Hg content in the roots and shoots was determined using ICP-MS, and the results are shown in Fig. 4. As observed from Fig. 4, the Hg content in the roots decreased with the addition of Fe^{2+} in the pretreatment solutions. The Hg content in the roots exposed to IHg was higher than those exposed to MeHg at each Fe^{2+} level (Fig. 4a). The Hg content in the shoots exposed to MeHg was significantly higher than in the shoots exposed to IHg regardless of the formation of iron plaque (Fig. 4b). The addition of Fe^{2+} prominently decreased the Hg content in the shoots exposed to MeHg, whereas no obvious change was found with IHg exposure.

The species of Hg in rice tissues

The species of Hg in the rice tissues and nutrient solutions were analyzed by HPLC-ICP-MS. Hg^{2+} and CH_3Hg^+ were separated, identified and quantified by this method with a recovery above 80 % (Rahman and Kingston 2004; Rahman et al. 2009). The mean percentages of Hg^{2+} and CH_3Hg^+ in the tissues and nutrient solutions are shown in Fig. 5. When rice was exposed to

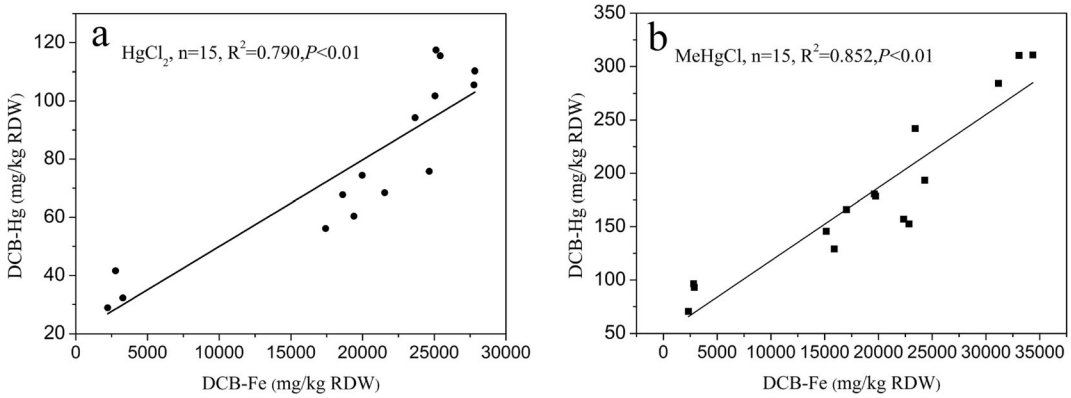

Fig. 3 Correlation between the Hg and Fe concentrations in the DCB extracts: $HgCl_2$ (**a**); MeHgCl (**b**) (RDW is the root dry weight)

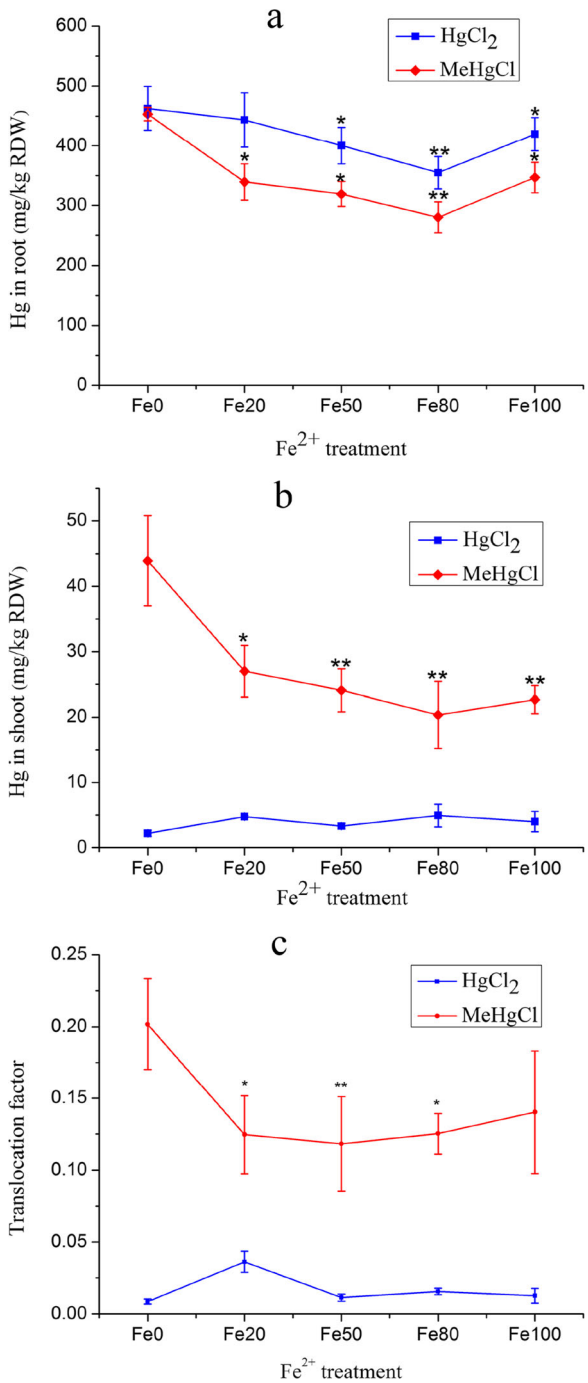

Fig. 4 Mean Hg content in roots (**a**) and shoots (**b**) and Hg translocation factor (**c**) in rice seedlings treated by different concentrations of Fe^{2+} and different species of Hg. Data are means±SD. (n=3) **p<0.01, *p<0.05 compared with Fe0 (control) group

IHg, the major specie of Hg in the rice roots was IHg, and MeHg was hardly detected in the tissues and nutrient solutions (Fig. 5a). Interestingly, when rice was exposed to MeHg, approximately 20 and 50 % of the Hg detected in the roots and shoots, respectively, were in the form of IHg (Fig. 5c). Meanwhile, no IHg was detected in the nutrient solutions with MeHg. The formation of iron plaque caused IHg to slightly increase in the roots and shoots of the rice exposed MeHg, but the amount was not significantly different (Fig. 5d).

The chemical forms of Hg in the rice tissues were analyzed with XANES. The main advantage of XANES over other methods is that it is less destructive and reflects information about the local molecular bonding environment of the element. The Hg L_3-edge XANES spectra of the roots exposed to both Hg species and the Hg reference compounds are shown in Fig. 6. The Hg L_3-edge spectra of $HgCl_2$ and MeHgCl exhibited a shoulder peak at 12284 eV, while root samples did not have such a shoulder peak. This result indicated that the Hg in the roots might interact with S rather than Cl.

The least-squares fit results of the root samples are shown in Table 1. When rice was exposed to IHg, most of the chemical forms of Hg were similar to $Hg(GS)_2$, accounting for approximately 78.5 % of the total Hg, and the others were similar to $HgCl_2$ and HgS. When rice was exposed to MeHg, the chemical forms of Hg were mainly similar to $Hg(GS)_2$ and CH_3HgGS. The corresponding proportion of $Hg(GS)_2$ and CH_3HgGS was approximately 1:4. In addition, the formation of iron plaque did not change the chemical forms of Hg in the rice tissues.

Discussion

The formation of iron plaque and IHg and MeHg adsorption in iron plaque

The basal part of the rice root releases O_2 (Fu et al. 2010), which causes the formation of Fe and Mn oxide and precipitation on the root surface. The formation of iron plaque was found to have a significant correlation with the rates of radial oxygen loss (ROL) in rice plants (Li et al. 2011; Wu et al. 2012; Yang et al. 2014).

Fe oxides play an important role in the cycle of Hg in aquatic ecosystems because of the strong adsorption and co-precipitation between Hg and Fe oxides (Fagerström and Jernelöv 1972). This study found that both IHg and MeHg, especially MeHg, could be adsorbed by iron

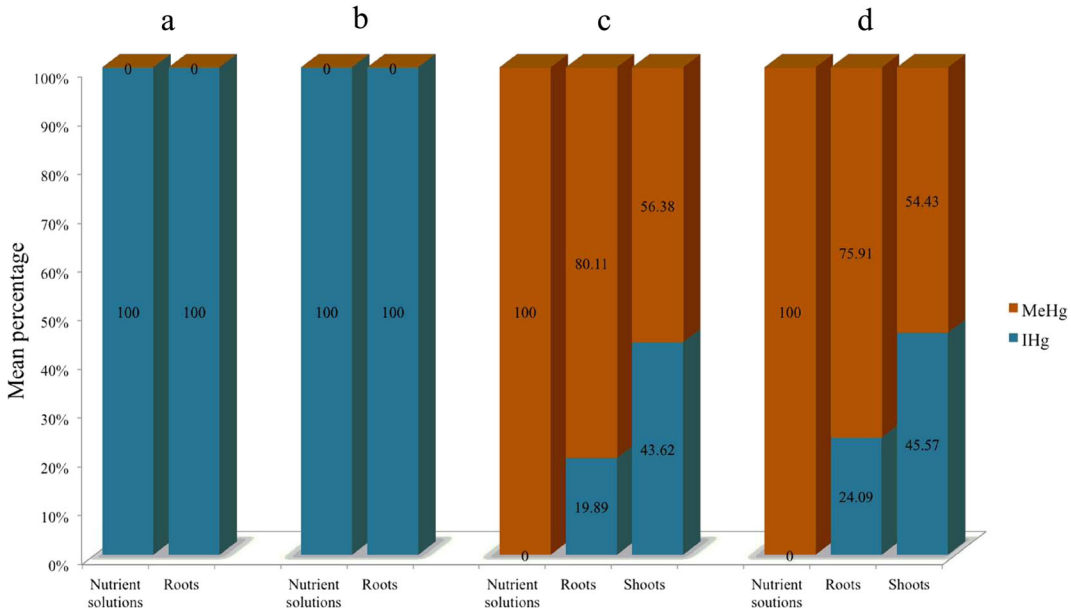

Fig. 5 The mean percentage of Hg^{2+} and CH_3Hg^+ in nutrient solutions and rice roots measured by HPLC-ICP-MS. **a** Rice without iron plaque induction under IHg exposure; **b** rice with iron plaque induction under IHg exposure; **c** rice without iron plaque induction under MeHg exposure, **d** rice with iron plaque induction under MeHg exposure

plaque. The Hg adsorption in the iron plaque had a positive correlation with the amount of iron plaque (Fig. 3). This result suggests that the Hg accumulation in the iron plaque correlated significantly with the Hg speciation. This was also reported in other studies. For example, Huang et al. found that the antimony (Sb) concentration in the iron plaque on rice root surfaces treated with Sb(III) were significantly higher than on rice root surfaces treated with Sb(V) (Huang et al. 2012). The predominant species of Sb(III) in aqueous solution is $[Sb_2(C_4H_2O_6)_2]^{2-}$ units with two negative charges, while Sb(V) exists as $Sb(OH)_6^-$ at pH>3 with one negative charge. Liu et al. (2005) found that arsenate was more easily absorbed by iron plaque than arsenite. The predominant species of arsenate and arsenite in solution were $H_2AsO_4^-$ and $H_3AsO_3^0$ at pH>3, respectively. It seems that the accumulation of Sb and As in iron plaque is closely linked to the quantity of the electric charge of their chemical forms in solution. $HgCl_2$ and CH_3HgCl are weak electrolytes. The dissociation constant of CH_3HgCl (pK=5.25) is higher than that of $HgCl_2$ (pK1=6.74, pK2=13.22) (De Robertis et al. 1998; Dyrssen and Wedborg 1991). There are more free ions in the rhizosphere with the MeHg treatment than that with the IHg treatment under the same pH range, and this may be responsible for the different adsorption rates of iron plaque to MeHg and IHg.

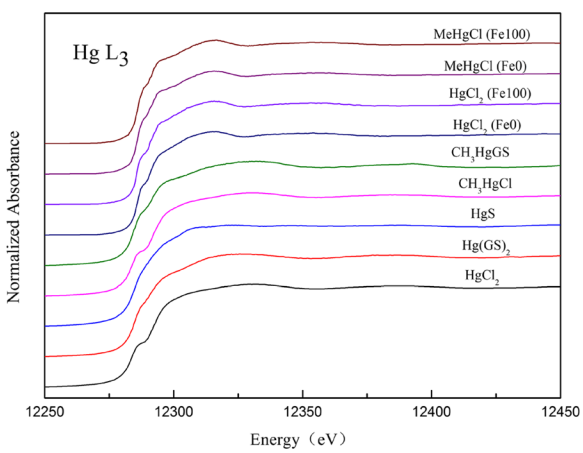

Fig. 6 Hg L_3 XANES spectra of the model compounds and the root samples of rice treated by different Hg species

Effects of iron plaque on the absorption and translocation of Hg

Iron oxides have high Hg adsorption and co-precipitation capacity. The addition of iron oxides significantly decreased the available Hg content in soil

Table 1 Percentage of Hg species in the IHg and MeHg-treated groups by least squares fitting. Values in parentheses show the SD

Sample	$HgCl_2$	$Hg(GS)_2$	HgS	CH_3HgCl	CH_3HgGS
$HgCl_2$ (Fe0)	22.0 (3.3)	78.7 (2.7)	<1	–	–
$HgCl_2$ (Fe100)	19.9 (2.0)	78.5 (3.9)	1.6(0.2)	–	–
MeHgCl (Fe0)	–	20.1 (6.4)	–	<1	79.1 (7.2)
MeHgCl (Fe100)	–	19.4 (7.5)	–	<1	80.0 (8.6)

(Ren et al. 2014). In order to exclude the possible effect of the Fe treatment on the Hg accumulation, the Fe^{2+} treatment solution was replaced by a normal nutrient solution after the iron plaque was induced, and then the rice seedlings were exposed to Hg in our experiment.

Hg was mainly concentrated in the epidermis, and endodermis, and the vascular tissues. The reason for this Hg distribution may be ascribed to the following: 1) the major cell wall structural proteins, such as extensins and expansins, contained characteristic cysteine-rich domains (McNear et al. 2012; Li et al. 2015). Because Hg has high affinity for the thiol groups in cysteine residues, it impaired the structure of the cell walls and aroused the deformation of the epidermal, cortical and xylem cells (Carrasco-Gil et al. 2013). 2) Hg ions could permeate into the inner root tissues via the apoplastic pathway in rice roots. Hg ions may also be transported across the plasma membrane of the endodermal barrier and enter the cell symplast, and they are then transported further to the central cylinder (Tester and Leigh 2001). Our results differ from a report on maize (*Zea mays* L.). Debeljak et al. (2013) found that Hg ions barely crossed the root plasma membranes of the endodermal barrier but were thoroughly restricted in the root apoplastic space in maize (*Zea mays* L.).

Iron plaque could actively inhibit the translocation of MeHg from roots to shoots, but this effect was not remarkable for IHg. Excess Fe^{2+} in the rhizospheric environment is toxic to the plant. It can inhibit the growth of the primary root (Ward et al. 2008). Therefore, appropriate levels of Fe^{2+} should be used to reduce Hg accumulation in rice plants.

The Hg content in the shoots exposed to MeHg was significantly higher than in the shoot exposed to IHg regardless of the formation of iron plaque (Fig. 4b). The translocation factor (TF) (Fig. 4c) was used as an indicator to evaluate the transfer ability of Hg from the roots to aboveground parts in rice. ($TF=T_{shoot\text{-}Hg}/T_{root\text{-}Hg}$, and $T_{shoot\text{-}Hg}$ and $T_{root\text{-}Hg}$ represent the Hg content in the shoots and roots, respectively.) The TF for the MeHg exposure was significantly higher ($p<0.05$) than that for the $HgCl_2$ exposure, indicating that MeHg was more easily transported from the roots to the shoots. The formation of iron plaque effectively inhibited the translocation of MeHg from the roots to the shoots. The result is consistent with other studies on Hg translocation in rice. Zhao et al. (2014) found that the proportion of MeHg over the total Hg increased from the roots to the grains, and MeHg can account for over 50 % of the total mercury in rice grains. On the contrary, the proportion of IHg decreased from the roots to the grains. Zhang et al. (2010) investigated the IHg and MeHg contents in rice grains from an Hg mining area and found that the bioaccumulation factors (BAFs) for MeHg were much higher than those for IHg in rice plants. Therefore, IHg and MeHg showed different accumulation abilities and distribution patterns in rice, implying that IHg and MeHg follow different absorption and translocation pathways in rice (Meng et al. 2014).

Methylation and demethylation of Hg and effects of iron plaque on Hg transformation

The result of the HPLC-ICP-MS showed that the chemical form of Hg in the rice roots was IHg when the rice was exposed only to IHg, suggesting that there was little or no methylation occurring in vivo in the rice seedlings (Fig. 5a). For the rice exposed to MeHg, approximately 20 and 50 % of the Hg detected in the roots and shoots, respectively, were in the form of IHg (Fig. 5c).

As is known, photochemical degradation is responsible for the MeHg demethylation in some freshwater lakes (Tai et al. 2014). Therefore, the photo-degradation of MeHg in the pretreatment solutions might be the source of IHg in the rice roots and shoots exposed to MeHg. To test this hypothesis, we examined the chemical forms of Hg in nutrient solutions. IHg was hardly detected in the nutrient solutions exposed to MeHg. These results suggested that demethylation could occur in rice roots.

Moreover, the proportion of IHg and MeHg was 1:4 in rice roots and 1:1 in shoots exposed to MeHg (Fig. 5c).

It has been confirmed that MeHg is transported more easily from the roots to aboveground parts than IHg. However, the proportion of IHg in the shoots was higher than that in roots when the rice seedlings were exposed to MeHg. A portion of the IHg comes from the demethylation of MeHg in the shoots. Hence, the demethylation of MeHg can occur not only in rice roots but also in shoots.

According to the Lewis acid–base theory, mercuric ions (Hg^{2+} or CH_3Hg^+) as soft Lewis acids had high affinities for thiolic groups that were soft Lewis bases. In this study, Hg was mainly in a form similar to Hg-GS upon exposure to IHg or MeHg. Wang et al. (2012) found that the Hg in *Brassica juncea* was bound to sulfur in a form similar to β-HgS (66–94 %), Hg-cysteine (1–10 %) and Hg-dicysteine (8–28 %). Carrasco-Gil et al. (2013) reported the use of an extended X-ray absorption fine structure (EXAFS) to study the Hg speciation in the roots of *Medicago sativa* (alfalfa). Their results revealed that root Hg was dominated by two similar forms, Hg-PC (40–46 %) and Hg-Cys ligand (30–38 %). XANES is strongly sensitive to the formal oxidation sate and coordination chemistry of the absorbing atom. However, this technique cannot distinguish among $Hg(Cys)_2$, $Hg(GS)_2$ and HgPCs because they provide very similar spectra (Carrasco-Gil et al. 2011). Therefore, these studies demonstrated that Hg exists in the form of R-S-Hg-S-R in rice roots, which is consistent with our results.

Phytochelatin (PCs) can form complexes with heavy metal ions in the cytosol to prevent metal ions from binding with proteins. These complexes are subsequently transported to the vacuoles (Salt and Rauser 1995). Therefore, PCs play a key role in plant tolerance to heavy metals, which also has been reported by Carrasco-Gil et al. (Carrasco-Gil et al 2011) in *Arabidopis thaliana*. They found that root growth inhibition was over 80 % in the cad2-1 (with low glutathione content) and cad1-3 (unable to synthesize PCs), whereas the wild-type was inhibited by only 35 % when Arabidopis thaliana was exposed to 10 μM Hg for 4 d (Carrasco-Gil et al 2011). GSH (γ-Glu-Cys-Gly) is a rich sulfur-containing tri-peptide with high affinity for Hg. However, Xiang et al. found that enhanced GSH concentrations did not increase metal resistance (Xiang et al 2001). Therefore, PCs are the major Hg-binding compounds in plants, and GSH plays a key role in metal stress tolerance by regulating plants to make PCs.

Moreover, from the result of XANES, most of the chemical forms of Hg were similar to RS-Hg-S-R and CH_3Hg-S-R under MeHg stress. The corresponding proportion of RS-Hg-S-R and CH_3Hg-S-R was approximately 1:4, which also indicated that demethylation could occur in vivo in rice seedlings.

The methylation of IHg and Hg^0 and the demethylation of MeHg are two important processes in the cycling of Hg in the environment (Li and Cai 2013). Our results showed that de-methylation can also occur in vivo in plants, and it may be a protective mechanism of rice against the phytotoxicity of MeHg. The mechanism of demethylation of MeHg and the factors influencing this process deserve further study. The formation of iron plaque had no evident effect on Hg transformation in rice plants with either the IHg or MeHg treatment (Fig. 5b, d) in this study, indicating that iron plaque may act as a functional 'physical barrier' for blocking MeHg and IHg uptake in rice.

Conclusions

Both Hg species, especially MeHgCl, could be adsorbed by iron plaque on the root surface. The formation of iron plaque reduced the $HgCl_2$ and MeHg uptake and significantly inhibited the MeHg translocation from the roots to the shoots in rice plants. The process of demethylation could occur in vivo in rice plants. The formation of iron plaque had no significant effect on the transformation of Hg.

Acknowledgments This work was supported financially by the National Natural Science Foundation of China (Grant Nos. 21377129, 21407150, U1432241). We thank all the staff at BL15U (SSRF) and BL1W1B (BSRF) for their assistance during the SRXRF and XAS measurements and data processing. Y-F Li gratefully acknowledges the support from the K. C. Wong Education Foundation, Hong Kong, and the CAS Youth Innovation Association, Chinese Academy of Sciences.

References

Benoit JM, Gilmour CC, Heyes A, Mason RP, Miller CL (2003) Geochemical and biological controls over methylmercury production and degradation in aquatic ecosystems. ACS Symp Ser 835:262–297

Carrasco-Gil S, Alvarez-Fernandez A, Sobrino-Plata J, Millan R, Carpena-Ruiz RO, Leduc DL, Andrews JC, Abadia J, Hernandez LE (2011) Complexation of Hg with phytochelatins is important for plant Hg tolerance. Plant Cell Environ 34:778–791

Carrasco-Gil S, Siebner H, LeDuc D, Webb SM, Millan Gomez R, Andrews JC, Hernandez L (2013) Mercury localization and speciation in plants grown hydroponically or in a natural environment. Environ Sci Technol 47:3082–3090

Clarkson TW, Magos L (2006) The toxicology of mercury and its chemical compounds. Crit Rev Toxicol 36:609–662

De Robertis A, Foti C, Patane G, Sammartano S (1998) Hydrolysis of CH_3Hg^+ in different ionic media: Salt effects and complex formation. J Chem Eng Data 43:957–960

Debeljak M, van Elteren JT, Vogel-Mikus K (2013) Development of a 2D laser ablation inductively coupled plasma mass spectrometry mapping procedure for mercury in maize (*Zea mays* L.) root cross-sections. Anal Chim Acta 787:155–162

Deng G, Zhang T, Yang L, Wang Q (2013) Studies of biouptake and transformation of mercury by a typical unicellular diatom Phaeodactylum tricornutum. Chin Sci Bull 58:256–265

Diez S (2009) Human Health Effects of Methylmercury Exposure. In: DM Whitacre (ed) Rev Environ Contam Toxicol 198: 111–132

Dyrssen D, Wedborg M (1991) The sulfur-mercury (II) system in natural-waters. Water Air Soil Pollut 56:507–519

Fagerström T, Jernelöv A (1972) Some aspects of the quantitative ecology of mercury. Water Res 6:1193–1202

Fu Y, Yu Z, Cai K, Shen H (2010) Mechanisms of iron plaque formation on root surface of rice plants and their ecological and environmental effects: a review. Plant Nutr Fert Sci 16: 1527–1534

He C, Liu X, Zhang F (2004) Formation of iron plaque on root surface and its effect on plant nutrition and ecological environment. J Appl Ecol 15:1069–1073

Horvat M, Nolde N, Fajon V, Jereb V, Logar M, Lojen S, Jacimovic R, Falnoga I, Qu LY, Faganeli J, Drobne D (2003) Total mercury, methylmercury and selenium in mercury polluted areas in the province Guizhou, China. Sci Total Environ 304:231–256

Hu Y, Huang Y, Huang Y, Liu Y (2013) Formation of iron plaque on root surface and its effect on Cd uptake and translocation by rice (*Oryza sativa L.*) at different growth stages. J Agro-Environ Sci 32:432–437

Hu Y, Huang YZ, Liu YX (2014) Influence of iron plaque on chromium accumulation and translocation in three rice (*Oryza sativa L.*) cultivars grown in solution culture. Chem Ecol 30:29–38

Huang Y, Chen Z, Liu W (2012) Influence of iron plaque and cultivars on antimony uptake by and translocation in rice (*Oryza sativa L.*) seedlings exposed to Sb(III) or Sb(V). Plant Soil 352:41–49

Jiang GB, Shi JB, Feng XB (2006) Mercury pollution in China. Environ Sci Technol 40:3672–3678

Khan M, Wang F (2009) mercury-selenium compounds and therie toxicological significance: woward a molecular understanding of the mercury-selenium antasonism. Environ Toxicol Chem 28:1567–1577

Lee C-H, Hsieh Y-C, Lin T-H, Lee D-Y (2013) Iron plaque formation and its effect on arsenic uptake by different genotypes of paddy rice. Plant Soil 363:231–241

Li YB, Cai Y (2013) Progress in the study of mercury methylation and demethylation in aquatic environments. Chin Sci Bull 58:177–185

Li P, Feng XB, Qiu GL (2010) Methylmercury exposure and health effects from rice and fish consumption: a review. Int J Environ Res Public Health 7:2666–2691

Li H, Ye ZH, Wei ZJ, Wong MH (2011) Root porosity and radial oxygen loss related to arsenic tolerance and uptake in wetland plants. Environ Pollut 159:30–37

Li YY, Zhao JT, Gao YX, Li YF, Li B, Zhao YL, Chai ZF (2014) Effects of iron plaque and selenium on the absorption and translocation of inorganic mercury and methylmercury in rice (*Oryza staiva* L.). Asian J Ecotoxicol 9:972–977

Li YF, Zhao JT, Li YY, Li HJ, Zhang J, Li B, Gao YX, Chen CY, Luo M, Huang R (2015) The concentration of selenium matters: a field study on mercury accumulation in rice by selenite treatment in Qingzhen, Guizhou. Plant Soil 391: 195–205

Liu W-J, Zhu Y-G, Smith FA (2005) Effects of iron and manganese plaques on arsenic uptake by rice seedlings (*Oryza sativa L.*) grown in solution culture supplied with arsenate and arsenite. Plant Soil 277:127–138

Liu H, Zhang J, Christie P, Zhang F (2008) Influence of iron plaque on uptake and accumulation of Cd by rice (*Oryza sativa L.*) seedlings grown in soil. Sci Total Environ 394: 361–368

Liu C, Chen C, Gong X, Zhou W, Yang J (2014) Progress in research of iron plaque on root surface of wetland plants. Acta Ecol Sin 34:2470–2480

McNear DH Jr, Afton SE, Caruso JA (2012) Exploring the structural basis for selenium/mercury antagonism in Allium fistulosum. Metallomics 4:267–276

Meng M, Li B, Shao J-j, Wang T, He B, Shi J-b, Ye Z-h, Jiang G-b (2014) Accumulation of total mercury and methylmercury in rice plants collected from different mining areas in China. Environ Pollut 184:179–186

Qiu GL, Feng XB, Wang SF, Shang LH (2006) Environmental contamination of mercury from Hg-mining areas in Wuchuan, northeastern Guizhou, China. Environ Pollut 142:549–558

Rahman GMM, Kingston HM (2004) Application of speciated isotope dilution mass spectrometry to evaluate extraction methods for determining mercury speciation in soils and sediments. Anal Chem 76:3548–3555

Rahman GMM, Fahrenholz T, Kingston HMS (2009) Application of speciated isotope dilution mass spectrometry to evaluate methods for efficiencies, recoveries, and quantification of mercury species transformations in human hair. J Anal At Spectrom 24:83–92

Ren LY, Zhao M, Dong YL, Wang F, Gao XH, Pang X (2014) Adsorption effect of two kinds of iron oxides on available Hg in soil. Acta Sci Cirumst 34:749–753

Salt DE, Rauser WE (1995) Mg-ATP dependent transport of phytochelations across the tonoplast of oat roots. Plant Physiol 107:1293–1301

Syu C-H, Jiang P-Y, Huang H-H, Chen W-T, Lin T-H, Lee D-Y (2013) Arsenic sequestration in iron plaque and its effect on As uptake by rice plants grown in paddy soils with high contents of As, iron oxides, and organic matter. Soil Sci Plant Nutr 59:463–471

Syu C-H, Lee C-H, Jiang P-Y, Chen M-K, Lee D-Y (2014) Comparison of As sequestration in iron plaque and uptake by different genotypes of rice plants grown in As-contaminated paddy soils. Plant Soil 374:411–422

Syversen T, Kaur P (2012) The toxicology of mercury and its compounds. J Trace Elem Med Biol 26:215–226

Tai C, Li Y, Yin Y, Scinto LJ, Jiang G, Cai Y (2014) Methylmercury photodegradation in surface water of the Florida Everglades: importance of dissolved organic matter-methylmercury complexation. Environ Sci Technol 48:7333–7340

Tester M, Leigh RA (2001) Partitioning of nutrient transport processes in roots. J Exp Bot 52:445–457

Tripathi RD, Tripathi P, Dwivedi S, Kumar A, Mishra A, Chauhan PS, Norton GJ, Nautiyal CS (2014) Roles for root iron plaque in sequestration and uptake of heavy metals and metalloids in aquatic and wetland plants. Metallomics 6:1789–1800

Wang XY, Li YF, Li B, Dong ZQ, Qu LY, Gao YX, Chai ZF, Chen CY (2011) Multielemental contents of foodstuffs from the Wanshan (China) mercury mining area and the potential health risks. Appl Geochem 26:182–187

Wang JX, Feng XB, Anderson CWN, Wang H, Zheng LR, Hu TD (2012) Implications of mercury speciation in thiosulfate treated plants. Environ Sci Technol 46:5361–5368

Wang R, Feng X-B, Wang W-X (2013) *In Vivo* mercury methylation and demethylation in freshwater tilapia quantified by mercury stable isotopes. Environ Sci Technol 47: 7949–7957

Wang X, Li B, Tam N-Y, Huang L, Qi X, Wang H, Ye Z, Meng M, Shi J (2014) Radial oxygen loss has different effects on the accumulation of total mercury and methylmercury in rice. Plant Soil 385:1–13

Ward JT, Lahner B, Yakubova E, Salt DE, Raghothama KG (2008) The effect of iron on the primary root elongation of Arabidopsis during phosphate deficiency. Plant Physiol 147:1181–1191

Wei TB, Li JJ, Bai CB, Lin Q, Yao H, Xie YQ, Zhang YM (2013) A highly selective colorimetric sensor for Hg2+ based on a copper (II) complex of thiosemicarbazone in aqueous solutions. SCIENCE CHINA Chem 56:923–927

Wei Q, Nagi R, Sadeghi K, Feng S, Yan E, Ki SJ, Caire R, Tseng D, Ozcan A (2014) Detection and spatial mapping of mercury contamination in water samples using a smart-phone. ACS Nano 8:1121–1129

Wu C, Ye Z, Li H, Wu S, Deng D, Zhu Y, Wong M (2012) Do radial oxygen loss and external aeration affect iron plaque formation and arsenic accumulation and speciation in rice? J Exp Bot 63:2961–2970

Xiang CB, Werner BL, Christensen EM, Oliver DJ (2001) The biological functions of glutathine revisited in Arabidopsis transgenic plants with altered glutathione levels. Plant Physiol 126:564–574

Yang J, Tam NF-Y, Ye Z (2014) Root porosity, radial oxygen loss and iron plaque on roots of wetland plants in relation to zinc tolerance and accumulation. Plant Soil 374: 815–828

Zhang H, Feng XB, Larssen T, Shang LH, Li P (2010) Bioaccmulation of Methylmercury versus inorganic mercury in rice (*Oryza stavis* L.) grain. Environ Sci Technol 44:4499–4504

Zhao JX, Li Y-F, Liang J, Wang XY, Li B, Liu W, Dong ZQ, Qu LY, Gao YX, Chen CY (2009) Concentrations of heavy metals in some vegetables and their potential risks to human health in Guiyang and Wanshan areas. Asian J Ecotoxicol 4:392–398

Zhao JT, Li Y-F, Li YY, Gao YX, Li B, Hu Y, Zhao YL, Chai ZF (2014) Selenium modulates mercury uptake and distribution in rice (*Oryza sativa* L.), in correlation with mercury species and exposure level. Metallomics 6:1951–1957